Proceedings of the 35th European Safety and Reliability & the 33rd Society for Risk Analysis Europe Conference
Edited by Eirik Bjorheim Abrahamsen, Terje Aven, Frederic Bouder, Roger Flage, Marja Ylönen
 Published by Research Publishing, Singapore.
doi: 10.3850/978-981-94-3281-3_ESREL-SRA-E2025-P8653-cd

Seismic fragility curves for onshore wind turbines including effects of earthquake-induced landslides

Stefania Zimbalatti

Department of Structures for Engineering and Architecture, University of Naples Federico II, Naples, Italy.
E-mail: stefania.zimbalatti@unina.it

Fulvio Parisi

Department of Structures for Engineering and Architecture, University of Naples Federico II, Naples, Italy.
E-mail: fulvio.parisi@unina.it

Onshore wind turbines are key components of green and sustainable energy infrastructure in many countries, which are built to exploit wind energy and turn it into electricity. To maximize input energy, onshore wind turbines (OWTs) are typically placed in open areas or on the crest of slopes in mountainous regions. Nonetheless, those locations pose the risk of OWTs under geological hazards, such as earthquakes and landslides. This study presents a methodology for development of fragility curves of OWTs located on soil slopes subjected to earthquake-induced landslide hazard, accounting for damage due to slope instability on both underground electric power pipelines and superstructure. Different performance levels are quantitatively defined multiple engineering demand parameters and their thresholds to assess functional and structural damage to OWTs at both local and global spatial scales. To that aim, a detailed finite element model of a benchmark wind turbine developed by the National Renewable Energy Laboratory was developed in OpenSees software. After that a suite of seismic ground motion records was selected, permanent slope displacements were predicted and incremental dynamic analysis of the benchmark OWT was carried out to calculate seismic fragility of both the pipeline and superstructure. Results indicate a strong influence of slope geometry and soil properties on seismic fragility, emphasizing the significant impact of landslides in addition to ground shaking. While previous studies have examined OWT vulnerability to wind and seismic forces, they often treat these hazards separately and overlook their interaction with soil instability. This study highlights the underexplored yet critical role of earthquake-induced landslides in assessing the seismic risk of OWTs.

Keywords: Renewable energy, onshore wind turbines, NREL 5 MW reference wind turbine, multi-hazard assessment, earthquake-induced landslides, fragility analysis.

1. Introduction

Although onshore wind turbines (OTWs) are primarily designed to withstand forces generated by wind and seismic ground motion, the potential damaging effects of secondary earthquake events (such as landslides, soil fracture, and liquefaction) on wind turbines should not be overlooked. Earthquake-induced landslides can compromise the safety level of both the OTW superstructure and associated infrastructure, such as underground electric power pipelines, leading to serious damage and operational failures. This is of particular concern as the location of OTWs is often chosen in areas where they can maximize energy production, such as on slopes or in mountainous regions, which may also be prone to seismic activity. As a result, a deeper understanding of the impact of secondary seismic events is essential to ensure the reliability of OTWs.

Previous studies focused on the vulnerability of OTWs against wind and seismic ground motion only (Asareh et al. 2016). Specifically, those studies

considered the effects of wind and seismic forces separately, often overlooking the potential interaction between those hazards and the soil instability that may occur as a result of earthquake ground motion. However, the interaction between the activation of an earthquake-induced landslide can significantly increase damage due to ground motion, producing premature operational failure or even collapse. Cumulative damage to OTWs due to both ground shaking and landslide movements still needs to be explored, despite its critical importance in both hilly and mountainous regions.

This study aims to address this research gap by developing a methodology for seismic fragility assessment of onshore wind turbines located on the crest of slopes in earthquake-prone areas. The proposed fragility models incorporate both primary and secondary seismic effects, providing a more comprehensive evaluation of OTW seismic risk. These findings are expected to support the development of more resilient wind energy infrastructure, ensuring that wind turbines are better equipped to withstand the complex challenges posed by multiple geohazards.

2. Methodology

Seismic fragility functions are mathematical models that provide the conditional probability of exceeding prescribed performance levels (PLs), such as a structural or non-structural failure, given the level of a seismic intensity measure (IM). Seismic fragility can then be convolved with hazard and exposure to probabilistically estimate the level of risk within a spatio-temporal scale, such as a single structure or site and 1-year timeframe.

A reference turbine and a geographical location were selected for this study. Based on location and subsoil category (herein defined according to Eurocode 8 (CEN 2003)), fragility analysis is carried out taking into account only the superstructure (in case of subsoil category A, i.e. rock or very stiff soil) or also the underground electrical cables (in case of softer soils). At that point, the following loads on the structure are modelled: wind load and seismic ground motion. The former is simulated using the Normal Wind Profile (NWP) model proposed by IEC 61400-3 (2009), while a suite of real ground motions recorded after strong earthquakes is selected. The selection of ground motion records was based on magnitude, distance from the seismic source and local site conditions to ensure representativeness of the seismic hazard at the study location. Each ground motion record is characterized by a vector-valued IM consisting of peak ground acceleration (*PGA*) and peak ground velocity (*PGV*). Such IMs together with the slope's characteristics allow the prediction of peak co-seismic displacement using a predictive model proposed by Foutopolou and Pitilakis (2015, 2017). This model was selected due to its ability to estimate permanent slope displacements under strong seismic excitation, making it particularly relevant for slow-moving landslides affecting infrastructure stability. Seismic fragility of the selected wind turbine was evaluated with respect to four performance levels, three of which refer to the superstructure, while one refers to the electrical cables. Each fragility point

was derived under increasing *PGA*, subsequently allowing the fitting of a lognormal probability distribution to fragility data for development of fragility curves. In the following sections, the methodology used in this study is described in detail.

2.1. *Selection of benchmark turbine*

The 5-MW NREL wind turbine model is intended to serve as a standard model for conceptual studies of modern offshore and onshore wind turbines. The definition of that turbine is described in detail in the report published in the National Wind Technology Center (NWTC – see Jonkman et al. 2019). It is a conventional three-bladed, upwind, variable-speed, collective-pitch controlled horizontal axis wind turbine (WT). Key geometric and mass properties of NREL 5 MW WT are summarised in Table 1.

Table 1. Main geometrical and mass properties of NREL 5 MW WT.

Property	Value
Rotor diameter (D)	126 m
Rotor center of mass height (h_{hub})	90 m
Blade mass	17,740 kg
Hub mass	56,780 kg
Nacelle mass	240,000 kg
Rotor-Nacelle-Assembly (RNA) mass	350,000 kg
Rated power	5 MW

The adopted WT is supported by a tapered steel tower assumed to be fixed at the base. The geometrical properties of the tower are provided in Table 2.

Table 2. Main geometrical and mass properties of the support tower.

Property	Value
Tower height (H)	87.6 m
Tower base diameter	6.0 m
Tower base thickness	0.027 m
Tower top diameter	3.87 m
Tower top thickness	0.019 m

Although this study uses the NREL 5-MW wind turbine as a benchmark, its findings can be generalized to other turbine designs and foundations with some adjustments. The NREL 5-MW model represents modern large-scale turbines, but variations in blade count, pitch control, or size may affect dynamic behavior and performance under seismic or wind loads. Thus, while the conclusions apply to similar turbines, structural and aerodynamic modifications are needed for different configurations.

2.2. *Load modelling*

Since the primary focus of this study is to investigate the effects of earthquake-induced landslides, the dynamic complexity arising from the rotor operation and aerodynamic loads are idealised (De Risi et al. 2018; Ali et al. 2020). The dynamic force due to rotor vibrations is neglected, whereas wind loads are statically applied along the height of the tower and at the hub. By contrast, seismic loading is modeled in the dynamic regime as an acceleration time history. To account for uncertainties in soil properties, different subsoil categories (B, C, D) are considered, following Eurocode 8 (CEN 2003). Additionally, a sensitivity analysis is conducted to evaluate the effects of slope geometry variations, including changes

in slope inclination and the distance between the wind turbine and the slope crest. These variations provide a more comprehensive understanding of how different geotechnical and morphological conditions influence the response of the structure subjected to earthquake-induced landslides. All these loads and modelling assumptions are discussed in the following sub-sections.

2.2.1. *Wind load*

In accordance with ASCE/SEI 7-10 (2010) and IEC61400-3 (2009), the Normal Wind Profile (NWP) model is used to determine how wind speed varies with tower height. For a standard wind turbine class, the wind speed profile follows the power-law, as defined in Eq. (1), and is then converted into horizontal forces using Eq. (2), as follows:

$$V(z) = V_{hub} \cdot \left(\frac{z}{h_{hub}}\right)^{\alpha} \quad (1)$$

$$F(z) = 0.5 \cdot \rho_a \cdot V(z)^2 \cdot A(z) \quad (2)$$

In these equations, $V(z)$ denotes the mean wind speed, while V_{hub} refers to the reference wind speed, i.e. 15 m/s, acting at the center of the rotor/hub (IEC 61400-1 (2005)). The variable z represents the tower elevation, and h_{hub} is the turbine's hub height above the ground level, as listed in Table 1. Ultimately, α is taken as 0.2, $F(z)$ refers to transformed nodal wind forces, ρ_a is the air density (assumed to be 1.25 kg/m^3), and $A(z)$ reflects the tributary area of the elements. The impact of thrust forces on the rotor is also considered using a simplified approach, through the formulation proposed in Eq. (3) (Arany et al. 2017):

$$f_{hub} = 0.5 \cdot \rho_a \cdot V_{hub}^2 \cdot \pi \cdot R_T \cdot C_T \quad (3)$$

where f_{hub} is the wind thrust force on the rotor, R_T is the rotor radius, and C_T represents the thrust coefficient, which is evaluated as follows:

$$C_T = 3.5 \cdot V_r \cdot \frac{2V_r + 3.5}{V_{hub}^3} \quad (4)$$

This latter coefficient describes the efficiency with which a wind turbine converts wind kinetic energy into thrust force on the rotor. In Eq. (4), V_r stands for the rated wind speed, which is the wind speed for which the turbine is designed to operate optimally (Frohboese et al. 2010).

2.2.2. *Seismic input selection*

The seismic input for dynamic analysis should represent anticipated earthquake scenarios and must be compatibly selected. The uniform hazard spectra (UHS) pertinent to the seismically active site of L'Aquila, Italy, is considered to check the spectral compatibility of the records. This is a potential location for onshore wind farms, being made of many open areas. REXEL software (Iervolino et al. 2009) was used to select suites of recorded ground motions that approach a target spectrum.

2.3. *Evaluation of earthquake-induced landslide displacement*

To assess the permanent displacement D induced by the earthquake, models proposed by Fotopoulou and Pitilakis (2015, 2017) are implemented. Those researchers developed five distinct predictive models, utilizing either a single or multiple intensity measures (IMs) of seismic ground shaking. The

predictive model applied in this study is presented in Eq. (5):

$$ln(D) = -8.360 + 1.873\, ln(PGV) - 0.347\, ln\left(k_y/PGA\right) - 5.964k_y \pm 0.64\epsilon \quad (5)$$

This model enables the prediction of D based on PGA, PGV, and k_y, the latter of which is the yield acceleration of the slope. In Eq. (5), ϵ is the standard normally distributed variable with zero mean and unit standard deviation, whereas 0.64 is the logarithmic standard deviation. The yield acceleration of the slope, k_y, depends on both geometric and mechanical characteristics of the slope, the relative location of the wind turbine with respect to the slope, and the effects of gravity loads transmitted from the wind turbine to the slope. Five values of the parameter k_y were considered: $0.05g$, $0.10g$, $0.15g$, $0.20g$, and $0.25g$. For each k_y-value, 100 levels of PGA between 0 and $1g$ were considered. For each k_y and PGA value, 10^4 displacement realizations were randomly generated using the Monte Carlo method, in order to obtain a sample representative of the co-seismic displacement.

2.4. *Definition of performance levels*

To estimate the fragility of the wind turbine, performance levels should be defined based on different demand parameters of the turbine, relevant to different hazard levels ranging from emergency shutdown to total collapse and failure of the structure. The PLs assigned to the selected wind turbine are shown in Table 3.

Table 3. Performance levels assumed in the study.

PL	Description	Performance measure	Threshold
PL1	Large rotation on tower top	θ_{max}	0.5°
PL2	Yielding of electrical cable	ε_m	ε_y
PL3	Large top displacement	Δ	1.25% H
PL4	Instability of shell structure	Y	1

The selected performance thresholds are based on established industry standards and previous studies. The first performance level (PL1) is related to maximum chord rotation of the tower (θ_{max}). The capacity value of 0.5 degrees corresponds to the maximum rotation for which the turbine is switched off (De Risi et al. 2018). The second performance level (PL2) is associated with loss of electrical cables' functionality, evaluated by comparing the average axial strain of cable due to slope movement (ε_m) to the yield axial strain of the cable material (ε_y). The third performance level (PL3) is related to excessive displacements on top of the tower, as PL1 could cause a loss of energy efficiency. In modern utility scale wind turbines this case is also known as earthquake-induced emergency shutdown. Finally, the fourth performance level (PL4) is checked according to provisions of Eurocode 3 – Part 1-6 (CEN 2007), which deals with strength and stability of shell structures. In detail, Annex D of that code is used to calculate the design buckling stress for unstiffened cylindrical and truncated conical shells.

3. Fragility analysis

Interruption of wind turbine operation can be caused both by excessive displacement and rotation on top of the tower, but also by breakage of underground electrical cables used to transport energy. Therefore, seismic fragility analysis is performed on both the electrical cables embedded in the subsoil and the superstructure, considering both earthquake ground shaking and slope movements. Such analysis is discussed in the following sections.

3.1. *Fragility analysis of the wind turbine superstructure*

The analysis was carried out employing the OpenSees software (McKenna 2011), which allows simulating the behaviour of structural and geotechnical systems subjected to seismic input and other types of loads. The finite element model (Cheng et al. 2023; Lavassas et al. 2003) of the wind turbine was developed based on the reference model of the 5 MW NREL standard onshore turbine, as published by NWTC and described in Section 2.1. The structural model is shown in Figure 1, where the geometry of the tower can be observed, featuring a tapered tubular structure. To ensure the validity of the finite element model, a modal analysis was performed to verify natural frequencies and mode shapes of the wind turbine structure. The results of this analysis were compared with available data (Jonkman et al. 2019), confirming that the model accurately represents the dynamic behaviour of the turbine.

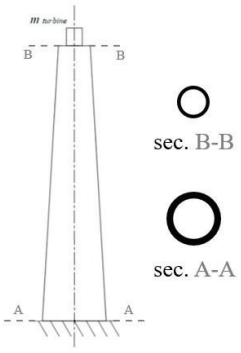

Fig. 1. Schematic representation of wind turbine model.

Once the model was validated, the analysis was carried out in two phases. The first phase involved applying wind loads through a static analysis with force control. The second phase consisted of applying seismic input, followed by a nonlinear incremental dynamic analysis (IDA) to evaluate the structural performance under seismic actions. Seismic demand was calculated for each *PGA* level and compared to the capacity associated with each PL, allowing for the evaluation of whether each PL was exceeded.

3.2. *Fragility analysis of underground electric power pipelines*

Considering the model shown in Figure 2, which is representative of a wind turbine located upstream of the slope affected by the landslide, a parameter was used to evaluate the failure of underground electrical cables, namely, the average cable strain ε_m caused by slope movement. That strain was estimated as the ratio between the co-seismic displacement (D) calculated via Eq. (5) and a conventional turbine-slope distance (x_T). IDA was performed to assess the performance of the electrical cables.

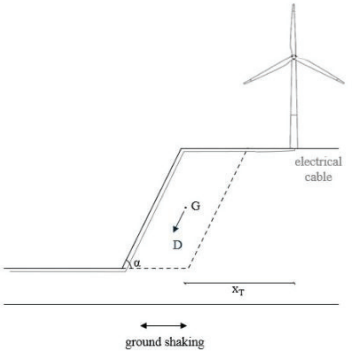

Fig. 2. Slope model considered in the study.

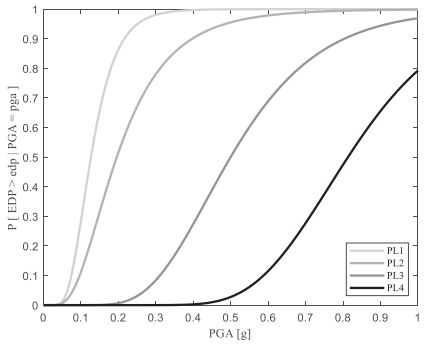

Fig. 3. Seismic fragility curves of the selected OTW.

4. Discussion of fragility curves

Given a prescribed value of critical acceleration k_y, which a representative parameter of seismic slope capacity, the conditional probability of exceeding a specific performance level given each *PGA* level was calculated as the ratio of the number of failure cases to the total number of simulations. This allowed for the determination of fragility based on the different *PGA* levels. A lognormal distribution was then fitted to fragility points to generate a fragility curve for each performance level. Figure 3 shows the fragility curves for all performance levels corresponding to $k_y = 0.05g$. Table 4 shows the median and standard deviation corresponding to each performance level.

Table 4. Median and standard deviation of seismic fragility curves.

Performance level	$\sigma_{\ln(PGA)}$	η_{PGA} [g]
PL1	0.41	0.13
PL2	0.55	0.19
PL3	0.37	0.50
PL4	0.25	0.81

It can be observed that, as expected, the fragility curves shift to the right as we move from the slight performance level to the collapse performance level. Additionally, the fragility curve associated with the performance level related to underground electrical cable rupture (PL2) is positioned close to the one related to large rotation on tower top (PL1). Meanwhile, the fragility curves corresponding to performance levels PL3 and PL4 are more closely associated with medium-to-high intensity seismic events. Considering these results, several mitigation strategies can be considered to improve the resilience of wind turbine, such as adopting structural reinforcements, optimising the design of underground cables to withstand slope movements, and integrating seismic dampers.

5. Conclusions

This study has proposed a methodology for developing seismic fragility curves for onshore wind turbines located on slopes subject to earthquake-induced landslides. The results obtained highlight the importance of considering the interaction between seismic ground motion and soil instability, which can significantly

influence the vulnerability of wind turbines and their associated infrastructure, such as underground electric power pipelines. The analysis showed that the slope geometry and soil characteristics play a crucial role in determining the seismic fragility of the wind turbine, suggesting the need for an integrated approach that simultaneously considers the risks from both earthquakes and landslides. This allows for a more accurate risk assessment and supports the design of more resilient turbines in vulnerable areas. Furthermore, the results of this study have important implications for wind farm site selection, emphasizing the need for a careful assessment of geological and seismic risks before choosing an area for turbine installation.

Acknowledgements

The work by the first author was supported by the Italian Ministry of University and Research, and Ten Project s.r.l., within the framework of Next Generation EU programme and the Italian National Plan for Recovery and Resilience. The study was also carried out within DPC-ReLUIS 2024–2026 project funded by the Italian Civil Protection Department.

References

Ali, A., De Risi, R., Sextos, A., Goda, K., and Chang, Z. (2020). Seismic vulnerability of offshore wind turbines to pulse and non-pulse records. *Earthquake Engineering and Structural Dynamics 49*, 24–50.

Arany, L., Bhattacharya, S., Macdonald, J., and Hogan, S.J. (2017). Design of monopiles for offshore wind turbines in 10 steps. *Soil Dynamics and Earthquake Engineering 92*, 126–152.

Asareh, M., Schonberg, W., and Volz, J. (2016). Fragility analysis of a 5-MW NREL wind turbine considering aero-elastic and seismic interaction using finite element method. *Finite Elements in Analysis and Design 120*, 57–67.

ASCE/SEI 7-10. Minimum Design Loads for Buildings and Other Structures: Second Printing 2010.

CEN. Eurocode 3: Design of steel structures – Part 1-6: Strength and Stability of Shell Structures. Comité Européen de Normalisation, Bruxelles, Belgium; 2007.

CEN. Eurocode 8: Design of structures for earthquake resistance – Part 1: General rules, seismic actions and rules for buildings. Comité Européen de Normalisation, Bruxelles, Belgium; 2003.

Cheng, Y., Luo, Y., Wang, J., Dai, K., Wang, W., and El Damatty, A. (2023). Fragility and vulnerability development of offshore wind turbines under aero-hydro loadings. *Engineering Structures 293*, 116625.

De Risi, R., Bhattacharya, S., and Goda, K. (2018). Seismic performance assessment of monopile-supported offshore wind turbines using unscaled natural earthquake records. *Soil Dynamics and Earthquake Engineering 109*, 154–172.

Fotopoulou, S.D., and Pitilakis, K.D. (2015). Predictive relationships for seismically induced slope displacements using numerical analysis results. *Bulletin of Earthquake Engineering 13*, 3207–3238.

Fotopoulou, S.D., and Pitilakis, K.D. (2017). Vulnerability assessment of reinforced concrete buildings at precarious slopes subjected to combined ground shaking and earthquake induced landslide. *Soil Dynamics and Earthquake Engineering 93*, 84–98.

Frohboese, P., and Schmuck, C. (2010). Thrust coefficients used for estimation of wake effects for fatigue load calculation. *European Wind Energy Conference.*

IEC 61400-1. Wind Turbines-Part 1: Design Requirements. Geneva, Switzerland: International Electrotechnical Commission; 2005.

IEC 61400-3. Wind Turbines-Part 3: Design Requirements for Offshore Wind Turbines. Geneva, Switzerland: International Electrotechnical Commission; 2009.

Iervolino, I., Galasso, C., and Cosenza, E. (2009). REXEL: computer aided record selection for code-based seismic structural analysis. *Bulletin of Earthquake Engineering 8*, 339–362.

Jonkman, J., Butterfield, S., Musial, W., and Scott, G. (2009). Definition of a 5-MW Reference Wind Turbine for Offshore System Development. *National Renewable Energy Lab.*

Lavassas, I., Nikolaidis, G., Zervas, P., Efthimiou, E., Doudoumis, I.N., and Baniotopoulos, C.C. (2003). Analysis and design of the prototype of a steel 1-MW wind turbine tower. *Engineering Structures 25*, 1097–1106.

McKenna, F. (2011). OpenSees: A framework for earthquake engineering simulation. *Computing in Science and Engineering 13*, 58–66.

Roy, T., and Matsagar, V. (2021). Multi-hazard analysis and design of structures: status and research trends. *Structure and Infrastructure Engineering 19*, 845–874.